

Amide modified polybutylene terephthalate: structure and properties

A. C. M. van Bennekom

GE Plastics, PO Box 117, 4600 AC Bergen op Zoom, The Netherlands

and R. J. Gaymans*

University of Twente, PO Box 217, 7500 AE Enschede, The Netherlands

(Received 7 December 1995; revised 3 May 1996)

Polyesteramide copolymers (PBTA) based on polybutylene terephthalate (PBT) and the diamide of butanediamine and dimethyl terephthalate (*N,N'*-bis(*p*-carbo-methoxybenzoyl)butanediamine) were studied. The amide content in PBTA was varied from 0–50 mol%. The melting and crystallization behaviour was analysed with differential scanning calorimetry. The degree of undercooling is taken as a measure for the rate of crystallization. The torsion modulus as a function of temperature and the position of the glass transition temperature (T_g) were studied with dynamic mechanical analysis. On injection moulded samples the tensile properties at RT were determined. The crystalline spacings were studied with wide angle X-ray diffraction. In the PBTA only one T_g could be observed which means that the amorphous phase was homogeneous. The crystalline spacings of PBT and Nylon 4,T were not the same and the PBTA has something of both, which means that the ester and amide repeat units are not isomorphous. Despite the absence of isomorphous crystallization the melting temperature increased nearly linearly with the amide content, the crystallinity remained high, and very surprisingly the rate of crystallization even increased. Also in polyethylene terephthalate these diamide segments increased the rate of crystallization. A model is proposed with the diamides as homogeneous nucleation sites (adjacent crystallization) to explain the fast crystallization behaviour of these copolymers. © 1997 Elsevier Science Ltd. All rights reserved.

(Keywords: polybutylene terephthalate; butanediamine; polyesteramides)

INTRODUCTION

Structurally regulated polyesteramides can be highly ordered copolymers, with properties intermediate of homopolymers. Polyamides are, in comparison with polyesters, characterized by higher glass transition (T_g) and melting (T_m) temperatures, better mechanical properties and a higher solvent resistance, but also a higher water sensitivity^{1,2}. This behaviour is mainly due to the intermolecular hydrogen bonding of the amide groups. It is expected that the incorporation of amide linkages in a polyester increases the interchain attraction and the stiffness of the polymer chains^{3,4}. Cocrystallization of ester and amide units in a polyesteramide generally requires isomorphism.

Alternating polyesteramides

Williams *et al.*⁵ have studied several alternating aliphatic–aromatic polyesteramides (nNTm), whereby n and m stand for the methylene length in respectively the diamine and the diol. The properties of the copolymers were intermediates of those of the two homopolymers showing a single T_g and T_m . Analysis by X-ray diffraction showed the presence of a single crystalline phase with a unit cell characteristic of the polyesteramide system and not of the individual polyamide or polyester units⁶. These alternating polyesteramides can thus be regarded as homopolymers.

The melting temperature decreased when the strictly alternating character was lost by ester–amide interchange^{7,8}.

Aharoni⁹ found liquid crystalline behaviour for alternating aliphatic–aromatic polyesteramides with an asymmetric chain structure. The presence of mesomorphicity depended on the length of the methylene spacer. Alternating polyesteramides containing short diamines with an even amount of methylene carbons did not show liquid crystalline phase behaviour.

Segmented copolymers with polyesteramide blocks

Preformed uniform diamide sequences have also been applied as a crystallizable block in thermoplastic elastomers (TPEs). The T_m and the T_g can be changed independently by varying the type and length of the crystalline and the amorphous segment. Gaymans and De Haan¹⁰ reported the synthesis of segmented polyether esteramide based on crystallizable diamide segments (1.5 repeating units of polybutylene terephthalamide, T4T) and polytetramethyleneoxide (PTMO). The T_m s and T_g s decreased with increasing amorphous block length, whereas the rate of crystallization remained high. The melting point depression of the crystallizable block was ascribed to a 'solvent' effect of the amorphous phase¹¹. Another example is a TPE based on T6T-segments (1.5 repeating units of polyhexamethylene terephthalamide) and PTMO-segments which had a melting temperature of 111°C¹².

*To whom correspondence should be addressed

Random polyesteramides with possible isomorphous structures

Random polyesteramides with diols and diamines of different methylene length and/or diacids with different methylene length, are not expected to show cocrystallization^{13,14}.

Random polyesteramides with diols and diamines of equal methylene length possess possible isomorphism, and cocrystallization seems feasible.

Ellis¹⁵ reported that blends of possible isomorphous poly(ϵ -caprolactone) (6E) and Nylon 6 (6A) were heterogeneous and showed immiscible phase behaviour. Random copolymers 6E/6A had a glass transition-composition relation inbetween linear additivity and the Fox relationship. However, thermal analysis of the polyesteramides revealed broad crystallization peaks and poorly defined melting endotherms. Goodman and coworkers¹⁶⁻¹⁸ observed that the crystal structures of the homopolymers (6E and 6A) were not isomorphous.

Other copolyesteramides with 'isomorphous' structures have been investigated¹⁹⁻²³. These random polyesteramides had apparently 'isomorphous' structures and a homogeneous amorphous phase (a single glass transition). Yet cocrystallization of the ester and amide units did not seem to occur and the crystallinity remained low.

Polyesteramides with uniform diamide units

Williams and Laakso²⁴ reported the synthesis of polyesteramides from preformed T6T, dimethyl, dimethyl terephthalate (DMT) and 1,6-hexanediol. These copolymers were based on polyhexamethylene terephthalate and polyhexamethylene terephthalamide (PHT/Nylon 6,T). The melting point was determined by polarized light microscopy and was taken as the temperature of complete disappearance of colour. It appeared that the melting temperature of the polyesteramide increased strongly with even low amide contents. The crystalline structure was found to be 'quite unlike unmodified terephthalate polyester', which indicates the occurrence of cocrystallization but not isomorphism. The patent did not mention randomization by ester-amide interchange reactions and a possible influence of non-uniformity of the length of the amide segment on the melting point.

Goodman and Starmer²⁵ reported the aggregation of uniform T6T segments in polyesteramides with aliphatic polyester blocks. Below about 25% T6T, the polymers remained amorphous and the polyester segment only crystallized by the application of stress.

Gaymans *et al.*²⁶ have reported the synthesis and properties of polyesteramides (PBTA) based on polybutylene terephthalate (PBT) and Nylon 4,T with the diamide of butanediamine and dimethyl terephthalate (*N,N'*-bis(*p*-carbo-methoxybenzoyl)butanediamine) (PBTA). The synthesis and thermal degradation of PBTA has also been further studied^{27,28}.

The T_g and T_m of PBTA increased with increasing amide content and its crystalline order and crystallization rate remained remarkably high compared to the homopolymer polybutylene terephthalate (PBT).

We studied the crystallization behaviour and some mechanical properties of PBTA, a PBT with 1,4-diaminobutane diamide units. Special attention is given to the influence of the purity (uniform length) of the 1,4-diaminobutane diamide units in the PBTA on the crystallization behaviour.

EXPERIMENTAL

Materials

PBTA samples were prepared from preformed diamide of butanediamine and dimethyl terephthalate (*N,N'*-bis(*p*-carbo-methoxybenzoyl)butanediamine, T4T, dimethyl), DMT and 1,4-butanediol²⁷. Before both processing and testing, the materials were dried at 100°C *in vacuo* overnight. PETA samples were prepared with ethylene glycol instead of butanediol. Polybutylene terephthalate (PBT) and polyethylene terephthalate (PET) were synthesized in the same way.

Processing

Torsion test bars were prepared on a Lauffer OPS 40 press at $T_m + 20^\circ\text{C}$. During 3-1-3 min a pressure of 0-3-10 bar respectively was applied. The mould was cooled at about $10^\circ\text{C min}^{-1}$ and the specimen was released. Tensile bars were injection moulded using an Arburg Allrounder 221-55-250. The temperature setting started at $T_m + 20^\circ\text{C}$, e.g. for PBTA10 (10 mol% amide) it was 250-260-270-270°C, with the mould at 90°C. The cycle consisted of 2 s injection at medium speed and 50 bar, 10 s hold at 35 bar and 20 s cooling time.

Viscometry

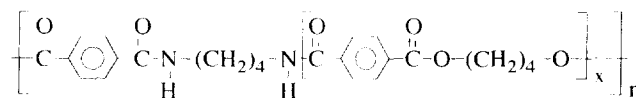
The inherent viscosity η_{inh} was determined at a 0.5 g dl^{-1} solution in phenol/1,1,2,2-tetrachloroethane (36/64 wt%) using a capillary Ubbelohde 1b placed in a water bath at $25.0 \pm 0.05^\circ\text{C}$.

Differential scanning calorimetry

For differential scanning calorimetry (d.s.c.) a Perkin Elmer DSC7 equipped with a PE-7700 computer and TAS-7 software was used, at a heating and cooling rate of $20^\circ\text{C min}^{-1}$ unless otherwise indicated. The peak maximum was taken as transition temperature and the area under the curve as enthalpy ΔH . About 4-8 mg of dry sample was heated to 20°C above its melting temperature (T_{m1}), after 1 min isothermal cooled (T_c) and heated again (T_{m2}). Tin was used as calibration standard.

Dynamic mechanical analysis

For dynamic mechanical analysis (d.m.a.) a Myrenne ATM3 torsion pendulum was used at a frequency of



PBTA

approximately 1 Hz. Samples of 70 mm length, 9 mm width and 2 mm thickness were monitored at a heating rate of $1^{\circ}\text{C min}^{-1}$. The T_g was defined as the maximum of the loss modulus G'' .

Tensile test

An Instron tensile apparatus was used at a strain rate of 5 mm min^{-1} . Test bars with $3 \times 6\text{ mm}^2$ cross section (ISO R527) were recorded at room temperature (r.t.). The modulus at 1% strain ($E_{1\%}$) and the maximum stress (σ_{max}) were determined from the stress-strain curve.

X-ray diffraction

Diffraction patterns at room temperature were obtained with a Philips powder wide angle X-ray diffractometer (WAXD), using nickel-filtered $\text{CuK}\alpha$ -radiation of 1.5418 \AA wavelength. Melt-pressed samples of 1 mm thickness were mounted in a sample holder perpendicular to the primary X-ray beam. A flat film Guinier-Simon camera with a sample-film distance of 90 mm was used to record the reflections at 2θ from 5 to 40° . The optical density data were collected from the photographed patterns using a linear scanning micro densitometer LS20.

RESULTS AND DISCUSSION

Glass transition

The glass transition indicates the temperature (range) at which chain segments start coordinated molecular motions²⁹. PBTA contains two types of units but appears to have one single T_g ²⁷. This suggests the presence of a homogeneous amorphous phase at least at microscale. The dependence of the T_g on the amide content in PBTA is approximately linear, from 47°C (for PBT) up to 160°C (for Nylon 4, T²⁶).

Melting temperature

The melting temperature of a copolymer is usually depressed compared to that of the homopolymers due to a lower crystalline order. This is explained in terms of non-isomorphism and randomization of the respective monomer units. Surprisingly, the melting temperature of PBT modified with uniform diamide units increases with increasing amide content (Figure 1)²⁶. The polyester-amides with 40 and 50 mol% amide melt pressed samples were only measured during a first heating scan in the d.s.c. It can be observed in Figure 1 that the melting transitions of the first and second heating scan hardly differed.

The increase in the melting temperature of these polyesteramides is non-linear, which indicates that random cocrystallization of ester and amide segments did not occur. Goodman and Vachon¹⁷ supposed that in case of random cocrystallization, the replacement of esters by amides (thus an increasing amide content) would lead to a formation of a hydrogen bonding system and hence to a gradual increase in T_m .

PBTA can probably not be regarded as homogeneously crystallizing, because as we have seen above, the structural isomorphism in polyesteramides does not seem to exist. If the crystallization is not random, it must be structured. Probably the diamide units in PBTA are ordered preferentially with other diamide units (on a nano-scale). This nano-ordering of the

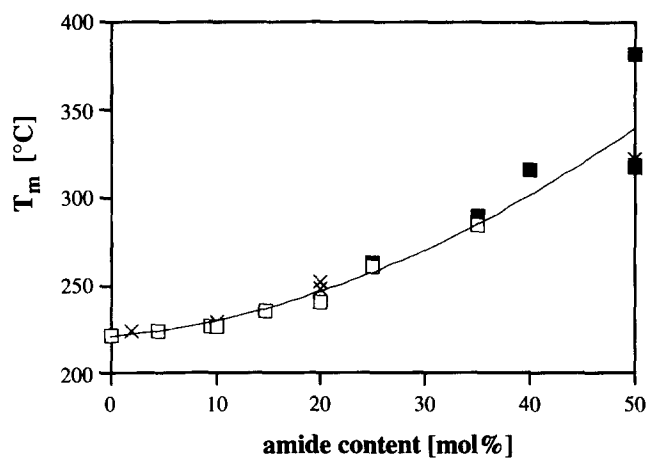


Figure 1 Melting temperature of PBTA versus amide content: ■, 1st heating scan²⁷; □, 2nd heating scan²⁷; ×, 2nd heating scan. PBTA from purified T4T.dimethyl

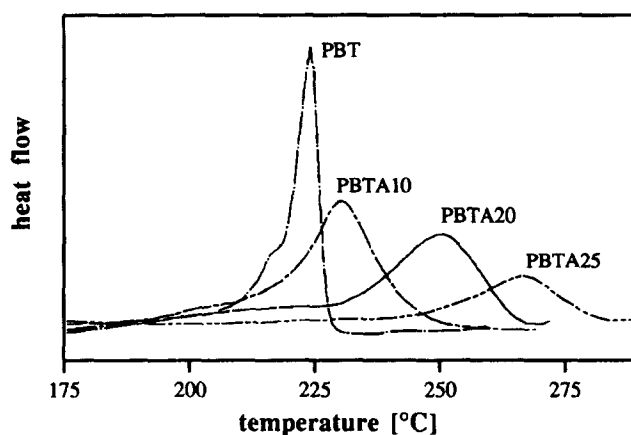


Figure 2 D.s.c., 2nd heating scan, showing the broadening of the melting peak with increasing amide content in PBTA

diamides in the melt will not restrict the crystallization of the ester units as long as their mobility is not changed. We now think that during cooling ester segments crystallize adjacent to the ordered diamide units. This ester-amide ordering can result in the observed increase of the melting temperature of PBTA with amide content (Figure 1).

The importance of a high degree of uniformity of the length of the amide segments to attain high melting temperatures has already been shown²⁸. In Figure 1 it can be observed for PBTA10 and PBTA20 that the use of purified (more uniform in length), T4T.dimethyl results in an increase of T_m . The presence of some longer amide segments may have caused a mismatch in the packing of diamides and with that of the whole crystalline phase. De Chirico³⁰ reported for alternating polyesteramide 6NT6 that the formation of amide blocks by ester-amide interchange lead to a decrease of the equilibrium melting temperature from 265 to 253°C .

Further, a broadening of the melting peaks with increasing amide content is observed in the d.s.c.-scans of the polyesteramides (Figure 2). The presence of a shoulder melting peak is not unusual for PBT and Nylon 6,6³¹⁻³³. This was attributed to a crystal rearrangement into a more stable lamellar organization. The broadness of the PBTA melting peak suggests the presence of a wide variety of lamellar sizes.

Rate of crystallization

The rate of crystallization is an important parameter for the melt processing of polymers. In the case of high crystallization rates, short cycle times can be used for injection moulding to attain semi-crystalline, dimensionally stable products. The crystallization temperature depends on the cooling rate. For PBT and PBTA02 (2 mol% amide) the influence of cooling rate on the d.s.c. traces is given in Figure 3.

The undercooling (ΔT) has been defined as the difference between the melting temperature (T_{m2}), measured at $20^\circ\text{C min}^{-1}$, and the crystallization temperature (T_c), measured at different cooling rates. This ΔT is a measure for the rate of crystallization. Bier *et al.*³⁴ found a linear relation of ΔT with the third root of the cooling rate. We have related the ΔT directly to the used cooling rate.

In Table 1, it is shown that the melting and crystallization temperatures of PBTA. PBTA02 and PBTA20 have lower ΔT values than PBT. The measured undercooling ΔT of PBTA has been related to the cooling rate (Figure 4a). The crystallization temperature of PBT and PBTA decreased about 20°C when the cooling rate

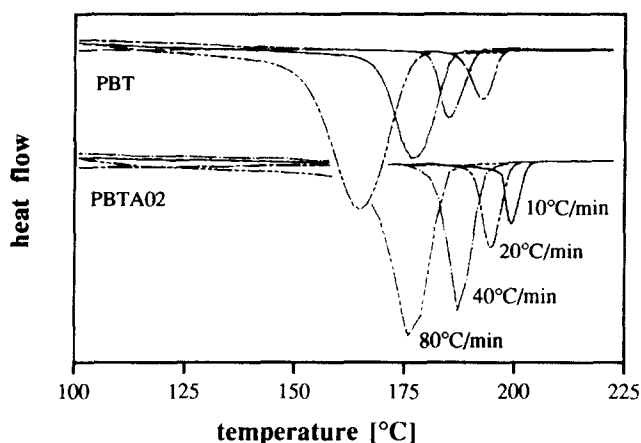


Figure 3 D.s.c., cooling scans of PBT and PBTA02 (2 mol% amide) vs cooling rate

increased from 20 to $80^\circ\text{C min}^{-1}$. At each cooling rate the ΔT of PBTA02 and PBTA20 is smaller than that of PBT. The PBTA02 with only 2 mol% of uniform diamides shows an unexpectedly large increase in the crystallization rate as compared to PBT.

For comparison PET has been modified with 2 mol% T4T.dimethyl ('PETA02'). This PETA02 was synthesized analogously to PBTA02. It is known that PET crystallizes extremely slow compared to its homologue PBT. The ΔT of PET is generally a factor of 2 larger than that of PBT (Table 1 and Figures 4a and 4b). However, the presence of 2 mol% diamide units (PETA02) appeared to decrease the ΔT of PET. The crystallization peak of modified PET (PETA02) was less broad and located at a higher temperature than that of PET.

The increase in crystallization rate for PETA02 compared to PET might partially be caused by a lower η_{inh} (Table 2)^{35,36}. However, after solid state postcondensation of PETA02, the η_{inh} increased, but the undercooling was hardly affected (Table 1).

The T4T units have accelerated the crystallization in the PBT copolymers (PBTA in Figure 4a) and in PET copolymers (PETA in Figure 4b). In the case of PBTA, the diamide units probably cocrystallize with the ester units. This results in increased melting temperatures with almost no change in the heat of melting. However, the

Table 1 Melting and crystallization temperatures of PBT and PET copolymers with T4T.dimethyl

Polymer	η_{inh} (dl g^{-1})	$20^\circ\text{C min}^{-1}$			$80^\circ\text{C min}^{-1}$	
		T_{m2}^a ($^\circ\text{C}$)	T_c ($^\circ\text{C}$)	ΔT ($^\circ\text{C}$)	T_c ($^\circ\mathbf{C}$)	ΔT ($^\circ\text{C}$)
PBT	1.39	222	186	36	164	58
PBTA02	1.02	217 + 224	191	32	173	51
PBTA20	1.01	249	219	30	200	49
PET	0.52	256	180	77	150	106
PETA02	0.32	237 + 254	191	63	160	94
PETA02 ^b	0.46	255	193	62	161	94

^a The main peak has been underlined

^b After solid state postcondensation (24 h at 225°C in N_2)

Table 2 Main wide-angle X-ray reflections of PBT, PBTA and Nylon 4,6 versus amide content (λ is 1.5418 \AA)

Sample	d_{100} (Å)	d_{010} (Å)	d_{001} (Å)	Remarks	Reference
PBT (α -form)	3.79	5.13	11.59	ρ 1.404 g cm^{-3} , relaxed	Yokouchi ⁴⁴
PBT (β -form)	3.71	5.19	12.95	ρ 1.283 g cm^{-3} , under stress	Yokouchi ⁴⁴
PBT	3.78	5.11	9.85	Valox 315	
PBTA10	3.75	5.11	10.1		
PBTA20	3.78	5.11	10.5		
PBTA20 ^a	3.83	5.18	10.5	highly non uniform	
PBTA30	3.85	5.04			Van Nieuwenhuize ³⁹
PBTA40	3.92	4.92			Van Nieuwenhuize ³⁹
PBTA50	3.90	4.93	10.7	4NT4	
Nylon 4,T	3.87	4.93	13.0 ^b , 13.2		
Nylon 4,6	3.87	4.14		melt pressed	Gaymans ⁴¹
Nylon 4,6 (α -form)	3.74	4.30		cast film triclinic	Gaymans ⁴²
Nylon 6,6 (α -form)	3.73	4.34			Masamoto ⁴³

^a Degraded PBTA20 (10 h at 270°C in *vacuo*)

^b Extrapolated value using data of Nylon 6,T and Nylon 8,T reported by Morgan and Kwolek⁴⁰

^c Reported by Brisson *et al.*⁴⁸

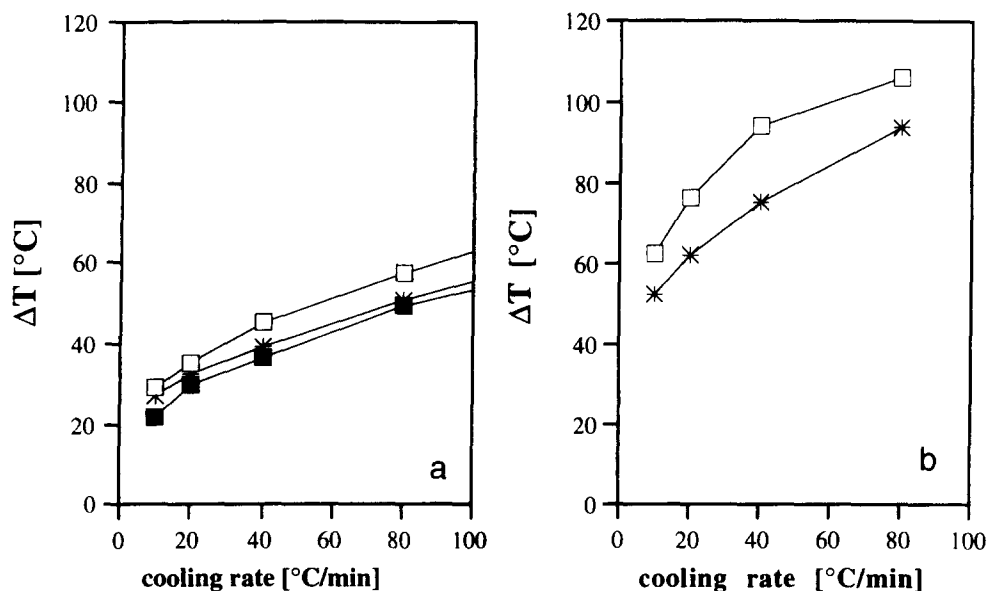


Figure 4 (a) Undercooling ΔT vs cooling rate: \square , PBT; *, PBTA02; \blacksquare , PBTA20. (b) Undercooling ΔT vs cooling rate: \square , PET; *, PETA02

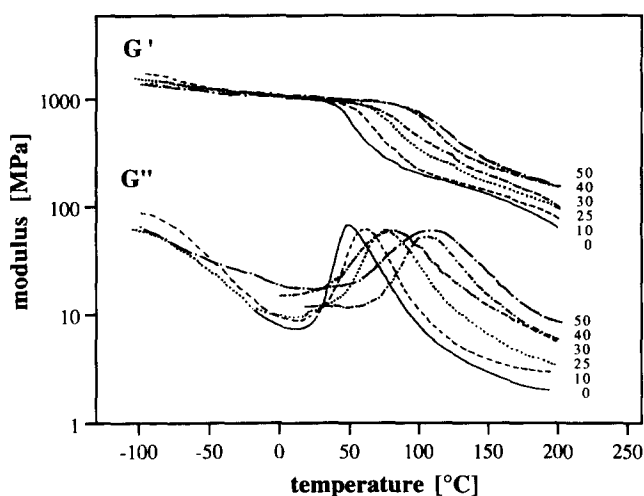


Figure 5 D.m.a. scans of dry PBT (0) and PBTA (10–50 mol% amide)²⁶

amide and ester repeat units in PETA are certainly non-isomorphous. A significant effect on the T_m of PETA02 compared to PET could not yet be observed (Table 1). The increase in the crystallization rate of PETA02 suggests that the uniform diamide segments (T4T) associate in the melt thereby acting as homogeneous crystallization nucleus. Yamada *et al.*³⁷ studied the effect of uniform segments of *p*-phenylene terephthalamide (T Φ T) on the crystallization of PET. However, these stiff diamide segments appeared to phase separate in the melt, and hampered the crystallization of PET.

Dynamic mechanical analysis

The viscoelastic properties of polyesteramides have been determined by a torsion pendulum test. The resistance against an applied torque was expressed as the storage modulus G' . The ratio of dissipated to potential energy was defined as the loss modulus G'' and a maximum of a G'' -temperature curve was defined as a glass transition (T_g). Figure 5 shows the influence of the ester-amide composition in PBTA on G' and G'' .

The T_g of the PBTA copolymer is a single transition

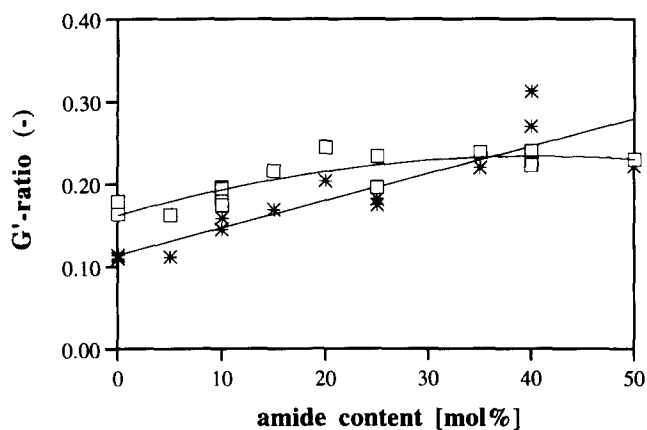


Figure 6 Ratio of G' moduli of dry PBTA versus amide content: \square , $G'(T_g + 50^\circ\text{C})/G'(T_g - 50^\circ\text{C})$; *, $G'(140^\circ\text{C})/G'(20^\circ\text{C})$

and shifts to higher temperatures with increasing amide content. This indicates that the amide and ester units form a homogeneous amorphous phase. The dissipation band in the G'' range is rather sharp for PBT and broadens with increasing amide content in PBTA.

The modulus of PBTA below the T_g is high and almost independent from the amide content. The modulus of PBTA above the T_g remains high due to the presence of the crystalline phase. This physical network is largely maintained up to the melting temperature of the polymer. The PBTA copolymers show high moduli at higher temperatures than PBT. The level of the modulus above the T_g is a function of the crosslink density and is for semi-crystalline polymers mainly controlled by the crystallinity and the size of the crystallites³⁶. In practice, the modulus at high temperature is often compared to the modulus at room temperature (20°C). In Figure 6 it is shown that the modulus ratio $G'(140^\circ\text{C})/G'(20^\circ\text{C})$ for PBTA increases with amide content. This implies that the G' modulus of polyesteramides shows a smaller decay with increasing temperature than observed for PBT.

Another way of looking at the data is to take the T_g as the ruling parameter. Therefore we have also calculated a

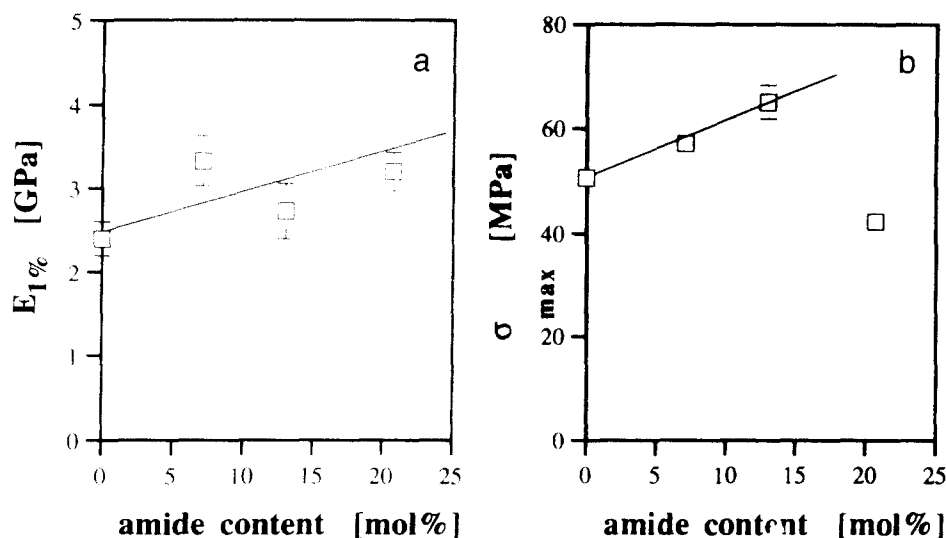


Figure 7 (a) Tensile modulus ($E_{1\%}$) of PBTA vs amide content (r.t., 12.5% per min). (b) Tensile strength (σ_{max}) of PBTA vs amide content (r.t., 12.5% per min)

ratio of moduli at 50°C above and below the T_g , $G'(T_g + 50^\circ\text{C})/G'(T_g - 50^\circ\text{C})$, for PBT and PBTA10/50 (Figure 6). The effect of the amide content on the latter modulus ratio of PBTA appeared to be less pronounced.

Nevertheless, the relative decrease of the G' modulus, corrected for the T_g , still shows an increase with amide content in PBTA. This effect is difficult to ascribe to a higher crystallinity, as the heat of melting of the PBTA samples with amide content of 20–50 mol% was not increased compared to PBT²⁶. Apparently, the presence of amide changes the crystallite structure in such a way that it improves the network function of the crystallites.

Tensile test

Stress-strain curves of polyesteramides were obtained by tensile tests at about 12.5% per min. In Figure 7a an increase of the modulus of polyesteramides with amide content is shown. At the temperature of testing (about 25°C) the stiffness of PBTA will be determined by the flexibility of the amorphous phase. Apparently, the PBTA copolymers have at 25°C a stiffer amorphous phase than PBT. The presence of amide segments in PBTA increases the interchain interaction compared to PBT. On the other hand, the lower modulus of PBT may also partly be ascribed to the fact that 25°C is near the glass transition of PBT (the T_g is 47°C, measured by d.m.a. at 1°C min⁻¹ and 1 Hz).

The tensile strength, shown in Figure 7b, also increases with amide content in PBTA. Evidently, the stress to break also depends on the degree of interchain interaction in PBTA. In general polyamides have a higher tensile strength than polyesters. In the case of the PBTA20 sample, fracture occurred before the yield stress was reached. This might have been due to the low molecular weight of the sample. The stiffness of polymers is, in general, little dependent on molecular weight.

Crystalline structure

In the X-ray diffraction pattern the sharp rings are from the crystalline phase and broad peak from the amorphous phase. The amorphous halo is for Nylon 6 at $2\theta = 21^\circ$. PET has two peaks at $2\theta = 17.5^\circ$ and 25° ³⁸.

A series of polyesteramides has been studied by X-ray with increasing amide content, from PBT up to PBTA50 (4NT4) and Nylon 4,T. The influence of the uniformity of the amides on the crystal structure was investigated with PBTA20 (Table 2). This sample was degraded at 270°C *in vacuo* during 10 h and contained an amide block fraction (X_{AA}/X_A) of 33%. In Table 2, the main wide angle X-ray reflections of the polyesteramides³⁹ are compared to those from PBT, Nylon 4,T⁴⁰, Nylon 4,6^{41,42} and Nylon 6,6⁴³. The calculations were limited to the interplanar spacings: d_{100} (in stacking direction or distance between parallel packed layers of terephthaloyl residues), d_{010} (the inter-planar distance in the direction of amide or ester bonding) and d_{001} (the period of identity along the chain axis).

The crystalline structure of PBT has been studied intensively and two triclinic crystalline configurations were found (an α form and a β form, Figure 8)^{44–46}. The transition between the two forms takes place reversibly by mechanical deformation: from the α form to the β form by elongation to about 12% or more and inversely by relaxation. The difference in fibre periods of the two crystalline forms is mainly ascribed to a conformational change of the four-methylene sequence in both forms (Figure 8). The β form has a larger period of identity and shows a larger density than the stable α form (Table 2).

The X-ray diffraction pattern of Nylon 4,T revealed a limited number of diffraction peaks^{47,48}. The crystalline structure is triclinic with an angle between the amide groups and benzene ring near to $\pm 30^\circ$. The Nylon 4,T chains are closer packed than in PBT due to the presence of hydrogen bonding and an all *trans* structure of the methylene sequence (Figure 8). This results in a much smaller d_{010} and a larger period of identity along the fibre axis: 13.2 Å for Nylon 4,T and 11.59 Å for PBT. A closer approach of the polymer chains, such as in Nylon 4,6 and Nylon 6,6 (Table 2) is hindered by the bulkiness of the terephthaloyl residue. Normally, the distance between the nitrogen and the oxygen in a hydrogen bond is in the range of 2.84 to 3.01 Å for Nylon *n*,T⁴⁸. This is larger than the N–O distance in aliphatic polyamides, e.g. about 2.8 Å in Nylon 6.

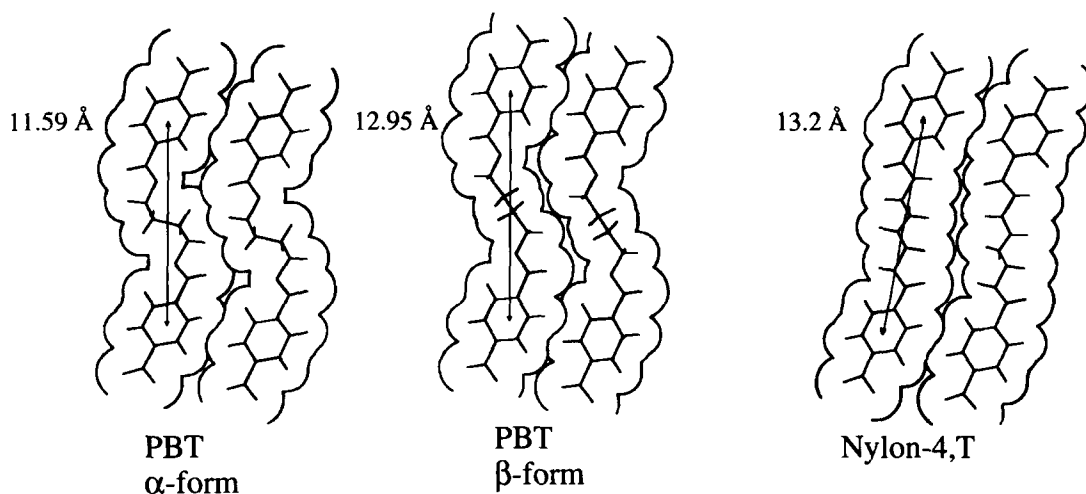


Figure 8 Molecular rearrangement in a crystal of PBT (α and β form) reported by Yokouchi⁴⁸ and in a crystal of Nylon 4,T (not reported, an all *trans* chain structure is assumed)

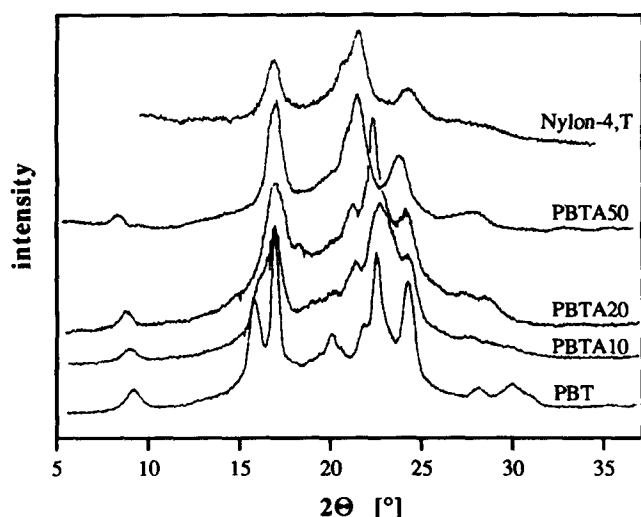


Figure 9 X-ray diffractograms of PBT, PBTA10, PBTA20, PBTA50 and Nylon 4,T (at r.t.)

In *Table 2* and *Figure 9*, it appears that PBTA10 and PBTA20 have about the same main d spacings as PBT. Thus, PBTA10 and PBTA20 may be crystallized in the α form of PBT. However, with increasing amide content, the PBT-reflections at 16.1° (d_{011}) and at 20.7° (d_{111}) shifted to the main peaks or became less pronounced. These reflections are related to the d_{001} spacing and indicate a change of the period of identity. The d_{001} itself increased with amide content, which points to a straightening of the chains. At higher amide content (PBTA30–50), the d_{010} decreased and the d_{100} increased compared to PBT and PBTA10–20.

PBTA40 and PBTA50 (4NT4) appeared to have the same crystal structure as Nylon 4,T. A crystallization of esters in the all *trans* structure of the polyamide may only be attained by stretching of the ester methylene sequence into the β -conformation of PBT. For PBTA50 the d_{010} spacing in the direction of the amide bonds was about equal to that of Nylon 4,T. Cesari *et al.*⁴⁹ also reported a planar zig-zag conformation for the alternating polyesteramide 6NT6. However, 6NT6 has a higher N–O distance (3.12 Å) than usually reported for Nylon n ,T (2.84–3.01 Å).

The sample with a high degree of non-uniformity (PBTA20#) has a larger unit cell size both for the d_{100} and d_{010} , which clearly indicates a poorer packing.

Crystallization process of PBTA20

Cocrystallization of the ester and amide monomer units in PBTA requires structural isomorphism of the PBT and Nylon 4,T repeating units. Allegra and Bassi⁵⁰ reported that isomorphism in a macromolecular system can be achieved when the respective units: (1) have about the same chain conformation and occupy the same volume; (2) are miscible in the amorphous phase.

The second requirement is met, since PBTA has a single glass transition and, therefore, a homogeneous amorphous phase. The melt of PBTA remained clear during polymerization which is another indication for the miscibility of the amorphous phase. However, the first requirement is not satisfied as the (triclinic) crystal structure of PBT and Nylon 4,T do not have the same unit cell dimensions (*Table 2*). Apparently PBT and Nylon 4,T are not isomorphous. The mismatch in conformation of the ester and amide units can hinder neighbouring ester–amide crystallization.

Therefore, we propose a structurally regulated crystallization process for the polyesteramides. In the case of PBTA20 the polymer chain contains T4T segments of more or less uniform length, separated by PBT-segments with an average of four repeating units. The lamellar crystallization of PBT is with an average thickness of four repeating units⁵¹. Van Hutten *et al.*¹¹ reported the occurrence of fast crystallization in segmented poly(ether esteramides) based on PTMO segments and crystallizable T4T segments. The very low undercooling ($T_m - T_c$) suggested order in the melt. Analogously, it can be assumed that the T4T segments in PBTA are also associated ('nano-ordered') in the melt.

We expect that PBTA20 crystallizes from a homogeneous melt, by ordering first the uniform diamide units; the ester units try to follow by adjacent ordering. The faster crystallizing T4T segments form the nuclei for the crystallization of the ester segments. In *Figure 10* this so-called amide-adjacent crystallization is schematized for PBTA20. This mechanism explains too why in PETA the T4T segments increase the crystallization rate (*Figure 4b*).

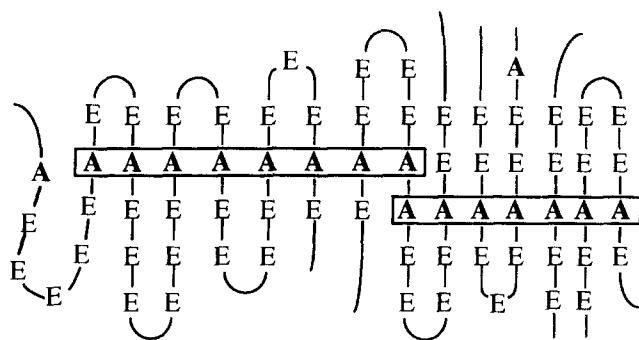


Figure 10 Proposed scheme for an amide-adjacent crystallization of PBTA20, showing the ordering of (uniform) diamide units and the disturbing effect of non-uniform amide segments

In case of a non-uniform length of an amide segment, the plane of hydrogen bonding in a lamella will be disturbed (*Figure 10*). In that region some dislocation of the hydrogen bond network is expected. X-ray diffraction of PBT and Nylon 4,T showed that their unit cells have a different size. Cocrystallization of ester and amide units in the indicated region is therefore not favourable. Thus, the presence of amide blocks disturbs the ordering process and probably also the lamellar dimensions in PBTA. With increasing amide block fraction, the melting temperature of PBTA20 decreased²⁹.

CONCLUSIONS

The properties of PBTA with uniform T4T segments have been studied. The T_g increased linearly with the amide content which indicated a homogeneous amorphous phase in PBTA. The melting point of the copolymers increased gradually with the amide content, although the crystalline structures of PBT and Nylon 4,T are not isomorphous (WAXD). We have proposed an amide-adjacent crystallization of PBTA in which the amides order first and the esters try to follow. The heat of melting in PBTA was not decreased compared to PBT, indicating that crystallization of the ester segments is not hindered significantly²⁶. The presence of amide segments of non-uniform length (amide blocks) depressed the melting temperature. This could be ascribed to a less perfect stacking of the non uniform segments in the lamellae.

The crystallization rate of PBTA copolymers increased compared to PBT. Surprisingly, the crystallization of PETA copolymers also occurred at a higher rate than PET homopolymer. These results affirm the existence of a nucleating effect of diamide units (T4T) in the polyesteramides.

The mechanical behaviour of PBTA was improved compared to PBT. The torsion modulus above the glass transition and the tensile modulus and strength at ambient temperature increased with increasing amide content. This improvement of mechanical properties was ascribed to the presence of stronger interactions in the crystalline and amorphous phase.

ACKNOWLEDGEMENTS

This research was financially supported by GE Plastics (Bergen op Zoom, The Netherlands). J. Bussink and J.

Feijen are acknowledged for the fruitful discussions and valuable suggestions. Alexej Turetskii is thanked for his contribution to the WAXD experiments.

REFERENCES

- 1 Korshak, V. V. and Vinogradova, S. V. in 'Polyesters', translated by B. J. Hazzard (Ed. J. Burdon), Pergamon, Oxford, 1965
- 2 Korshak, V. V. and Frunze, T. M. in 'Synthetic Hetero-chain Polyamides', translated by N. Kann, Monson, Jerusalem, 1964
- 3 Aubineau, C. and Champetier, G. *Bull. Soc. Chim. France* 1970, **4**, 1404
- 4 Sprague, B. S. and Singleton, R. W. *Tex. Res. J.* Nov. 1965, 999
- 5 Williams, J. L. R., Laakso, T. M. and Contois, L. K. *J. Polym. Sci.* 1962, **61**, 353
- 6 De Candia, F., Maglio, G. and Palumbo, R. *Polym. Bull.* 1982, **8**, 109
- 7 Williams, J. L. R., Carlson, J. M. and Reynolds, G. A. *Makromol. Chem.* 1963, **65**, 54
- 8 Borri, C., Sorta, E. and Zotteri, L. *Polymer* 1975, **16**, 565
- 9 Aharoni, S. M. *Macromolecules* 1988, **21**, 1941
- 10 Gaymans, R. J. and De Haan, J. L. *Polymer* 1993, **35**, 4360
- 11 Van Hutten, P. F., Mangnus, R. M. and Gaymans, R. J. *Polymer* 1993, **35**, 4193
- 12 Sorta, E. and Della Fortuna, G. *Polymer* 1980, **21**, 728
- 13 Castaldo, L., De Candia, F., Maglio, G., Palumbo, R. and Strazza, G. *J. Appl. Polym. Sci.* 1982, **27**, 1809
- 14 Goodman, I. *Eur. Polym. J.* 1984, **20**, 241
- 15 Ellis, T. S. *J. Polym. Sci., Polym. Phys. Edn* 1993, **31**, 1109
- 16 Goodman, I. and Vachon, R. N. *Eur. Polym. J.* 1984, **20**, 529
- 17 Goodman, I. and Vachon, R. N. *Eur. Polym. J.* 1984, **20**, 539
- 18 Goodman, I. *Eur. Polym. J.* 1984, **20**, 549
- 19 Goodman, I. and Sheahan, R. J. *Eur. Polym. J.* 1990, **26**, 1081
- 20 Goodman, I. and Sheahan, R. J. *Eur. Polym. J.* 1990, **26**, 1089
- 21 Tschang, Ch. J., Schollmeyer, E., Hirt, P. and Herlinger, H. *Angew. Makromol. Chem.* 1976, **52**, 143
- 22 Jasse, B. *Bull. Soc. Chim. France* 1965, 1640
- 23 Akçatel, P. and Jasse, B. *J. Polym. Sci., Polym. Chem. Edn* 1978, **16**, 1401
- 24 Williams, J. L. R. and Laakso, T. M. (Eastman Kodak, N.Y., USA), US Patent 2851443, 1958
- 25 Goodman, I. and Starmer, D. A. *Eur. Polym. J.* 1991, **27**, 512
- 26 Gaymans, R. J., De Haan, J. L. and Van Nieuwenhuize, O. *J. Polym. Sci., Polym. Chem. Edn* 1993, **31**, 575
- 27 Van Bennekom, A. C. M. and Gaymans, R. J., *Polymer* 1996, **37**, 5439
- 28 Van Bennekom, A. C. M., Willemsen, P. A. A. T. and Gaymans, R. J., *Polymer* 1996, **37**, 5447
- 29 Sperling, L. H. in 'An Introduction to Physical Polymer Science', 1985, Wiley, New York
- 30 De Chirico, A. *Eur. Polym. J.* 1978, **14**, 329
- 31 Hobbs, S. Y. and Pratt, C. F. *Polymer* 1975, **16**, 462
- 32 Nichols, M. E. and Robertson, R. E. *J. Polym. Sci., Polym. Phys. Edn* 1992, **30**, 305
- 33 Todoki, M. and Kawaguchi, T. *J. Polym. Sci., Polym. Phys. Edn* 1977, **15**, 1067
- 34 Bier, P., Binsack, R., Vernaleken, H. and Rempel, D. *Die Angew. Makromol. Chem.* 1977, **65**, 1
- 35 Van Antwerpen, F. Thesis 1971, TH Delft. G. J. Thieme, Nijmegen
- 36 Jadhav, J. Y. and Kantor, S. W. in 'Encyclopedia of Polymer Science' (Eds H. F. Mark, N. M. Bikales, C. G. Overberger, G. Menges and J. I. Kroschwitz), 2nd Edn, Vol. 12. Wiley, New York, 1988
- 37 Yamada, K., Harashimoto, K., Takayanagi, M. and Murata, Y. *J. Appl. Polym. Sci.* 1987, **33**, 1649
- 38 Murthy, N. S. and Minor, H. *Polymer* 1990, **31**, 996
- 39 Van Nieuwenhuize, O. Internal report UT, Enschede, 1985
- 40 Morgan, P. W. and Kwolek, S. L. *Macromolecules* 1975, **8**, 104
- 41 Gaymans, R. J. and Aalto, S. *J. Polym. Sci., Polym. Chem. Edn* 1989, **27**, 430
- 42 Gaymans, R. J., Van Utteren, T. E. C., Van den Berg, J. W. A. and Schuyer, J. *J. Polym. Sci., Polym. Chem. Edn* 1977, **15**, 537
- 43 Masamoto, J., Sasaguri, K., Ohizumi, C. and Kobayashi, H. *J. Polym. Sci., Polym. Phys. Edn* 1970, **8**, 1703
- 44 Yokouchi, M., Sakakibara, Y., Chatani, Y., Tadokoro, H., Tanaka, T. and Koda, K. *Macromolecules* 1976, **9**, 266

- 45 Nakamae, K., Kameyama, M., Yoshikawa, M. and
Matsumoto, T. *J. Polym. Sci., Polym. Phys. Edn* 1982, **20**, 319
- 46 Desper, C. R., Kimura, M. and Porter, R. S. *J. Polym. Sci.,
Polym. Phys. Edn* 1984, **22**, 1193
- 47 Gaymans, R. J. J. *J. Polym. Sci., Polym. Chem. Edn* 1985, **23**, 1599
- 48 Brisson, J., Gagné, J. and Brisse, F. *Can. J. Chem.* 1989, **67**,
840
- 49 Cesari, M., Perego, G. and Melis, A. *Eur. Polym. J.* 1976, **12**,
585
- 50 Allegra, G. and Bassi, I. W. *Fortschr. Hochpolymerforsch.* 1969,
6, 549
- 51 Adams, R. K. and Hoeschele, G. K. in 'Thermoplastic
Elastomers—A Comprehensive Review', Hanser, Munich,
1987, Chapter 8